# Excited State Dynamics of Bistridentate and Trisbidentate $Ru^{II}$ Complexes of Quinoline-Pyrazole Ligands

**SUPPORTING INFORMATION**

Lisa A. Fredin,[b,†,‡] Joachim Wallenstein,[a,‡] Elin Sundin,[a] Martin Jarenmark,[c] Deise F. Barbosa de Mattos,[a] Petter Persson,[b] Maria Abrahamsson,[a,*]

[a] Department of Chemistry and Chemical Engineering, Chalmers University of Technology, SE-41296 Gothenburg, Sweden

[b] Theoretical Chemistry Division, Department of Chemistry, Chemical Center, Lund University, Box 124, SE-22100 Lund, Sweden

[c] Department of Geology, Lund University, Solvegatan 12, SE-22362, Lund, Sweden

[†]Department of Chemistry, Lehigh University, 6 E Packer Avenue, Bethlehem, PA, 18015, USA

Author Contributions

[‡]These authors contributed equally. *abmaria@chalmers.se

## TEMPERATURE DEPENDENT ABSORPTION SPECTRA

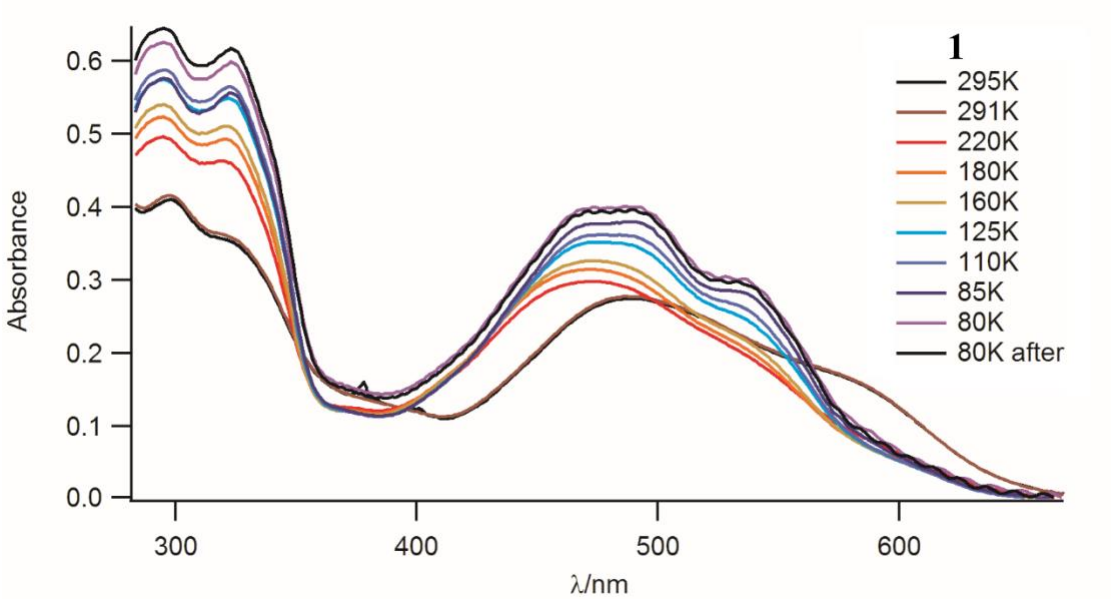


**Figure S1.** Temperature dependence of absorption spectra of **1** in MeOH:EtOH mixture (1:4) (Not corrected for volume change).

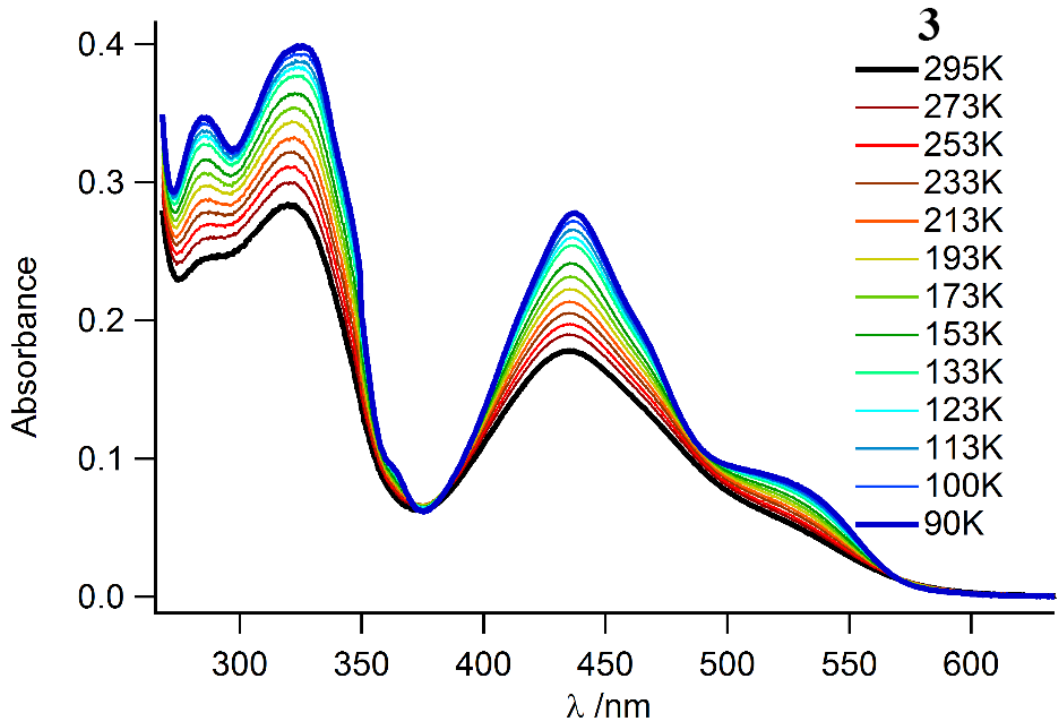


**Figure S2.** Temperature dependence of absorption spectra of **3** in MeOH:EtOH mixture (1:4) (corrected for volume change)

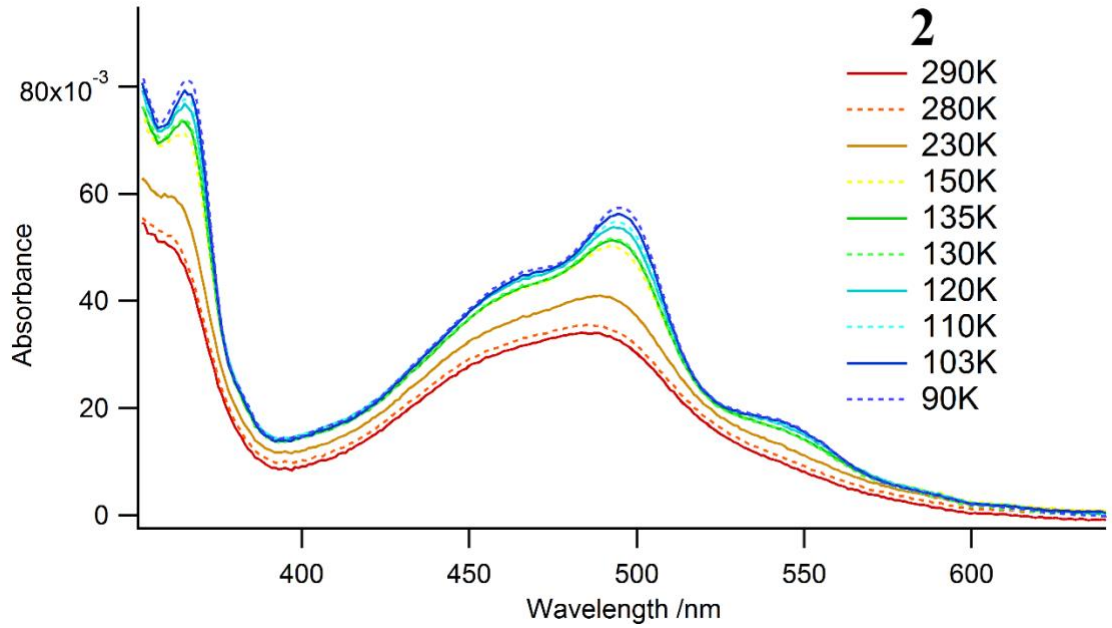


**Figure S3.** Temperature dependence of absorption spectra of **2** in MeOH:EtOH mixture (1:4) (Not corrected for volume change).

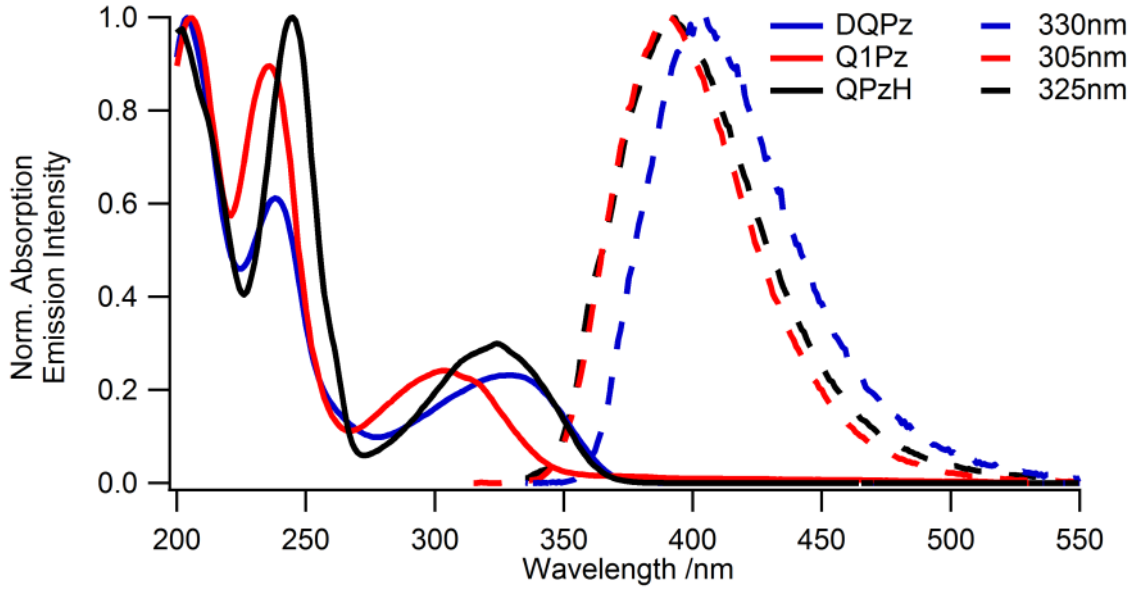


**Figure S4.** Absorption (solid) and emission (dashed) spectra of ligands Q3PzH, Q1Pz, and DQPz in neat acetonitrile. Excitation wavelength indicated in legend.

**LOW TEMPERATURE EMISSION SPECTRA**

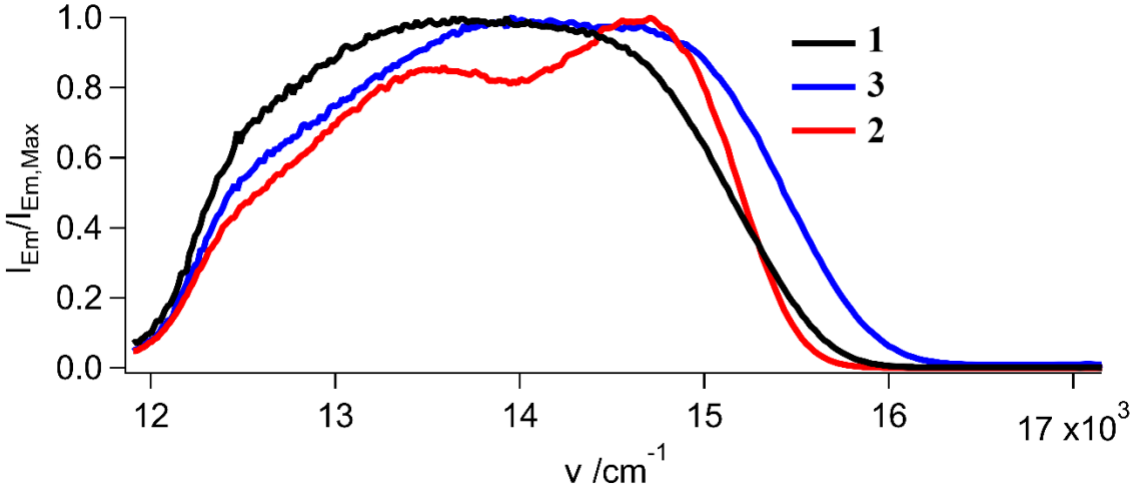


**Figure S5.** Corrected emission spectra in wavenumbers of **1**, **3**, and **2** in MeOH:EtOH glass at 77 K excited at the MLCT maxima with 475, 450, and 495 nm light respectively. Detailed temperature study in Figures S6-S8. Extinction coffecients for all of the complexes have been published in ref 23.

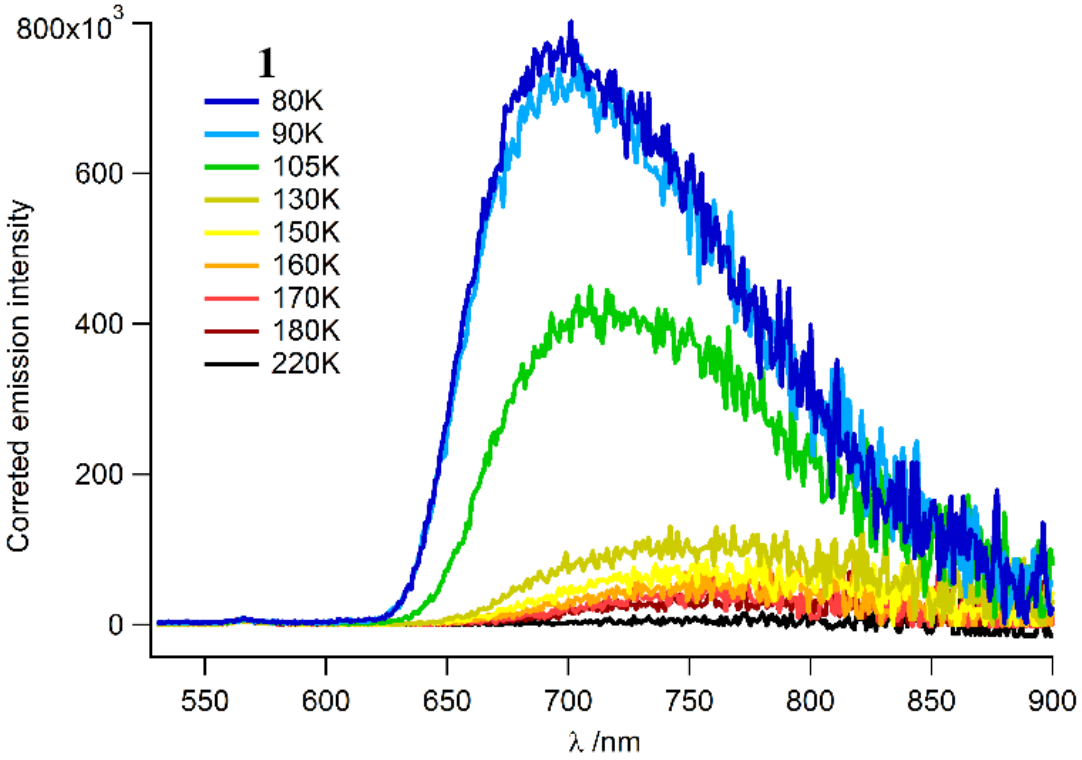


**Figure S6.** Temperature dependence of corrected emission spectra of **1** in MeOH:EtOH mixture (1:4) excited at the MLCT maxima with 445 nm light.

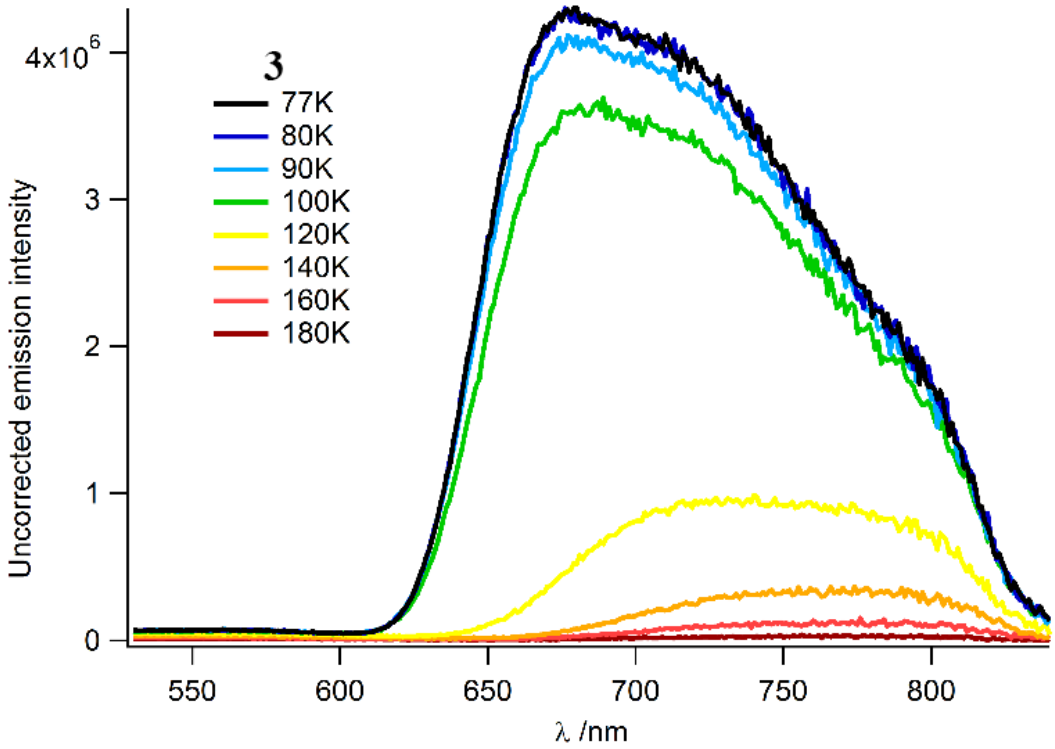


**Figure S7.** Temperature dependence of Uncorrected emission spectra of **3** in MeOH:EtOH mixture (1:4) excited at the MLCT maxima with 435 nm light.

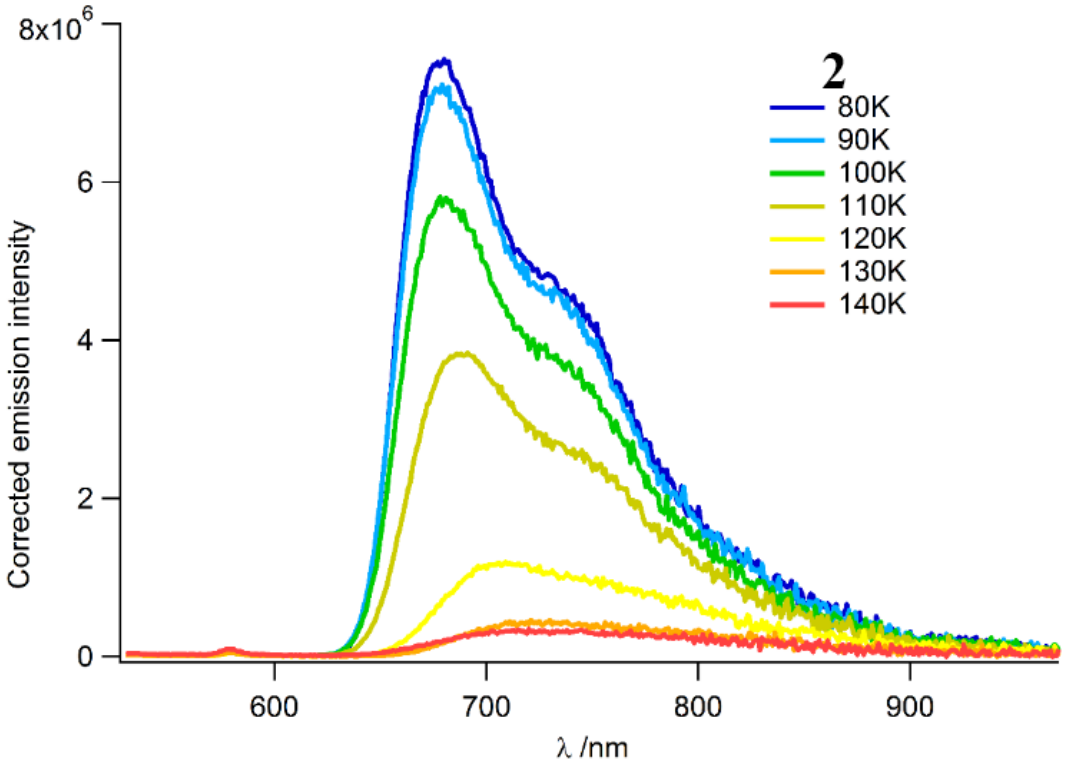


**Figure S8.** Temperature dependence of corrected emission spectra of **2** in MeOH:EtOH mixture (1:4) excited at the MLCT maxima with 495 nm light.

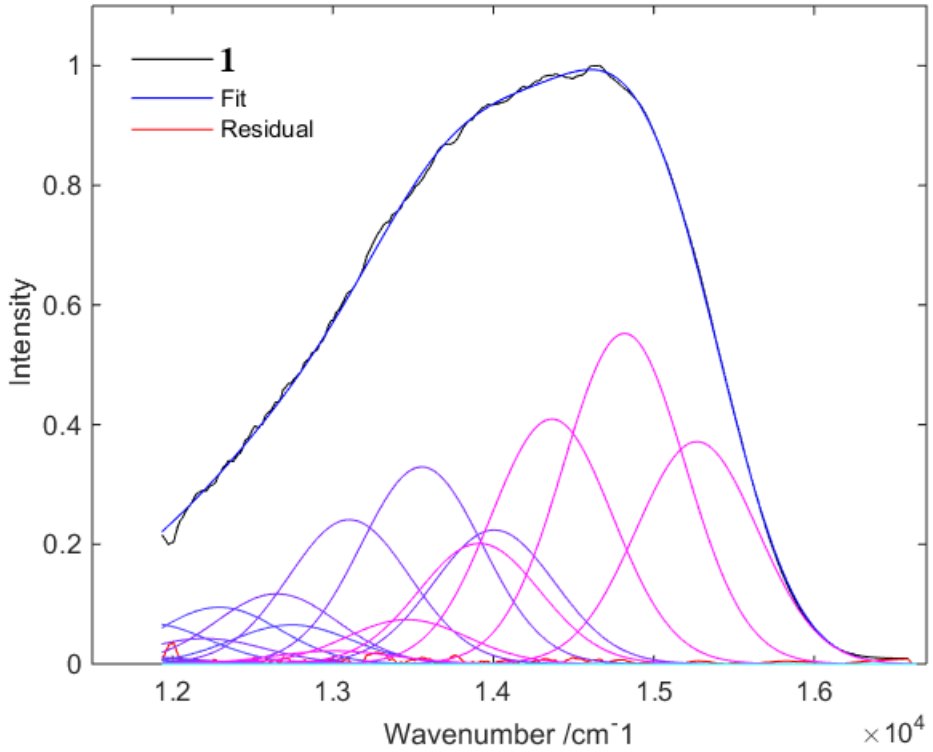


**Figure S9.** Spectral component analysis for **1** in MeOH:EtOH (1:4) glass at 77K excited at the MLCT maxima with 475 nm light.

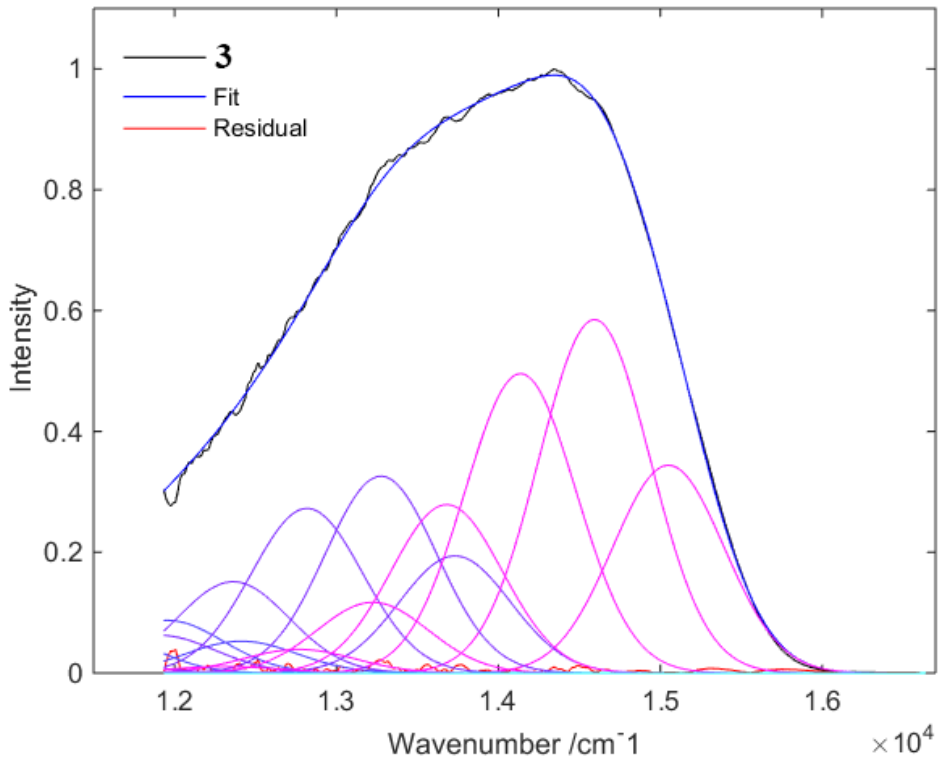


**Figure S10.** Spectral component analysis for **3** in MeOH:EtOH (1:4) glass at 77 K excited at the MLCT maxima with 450 nm light.

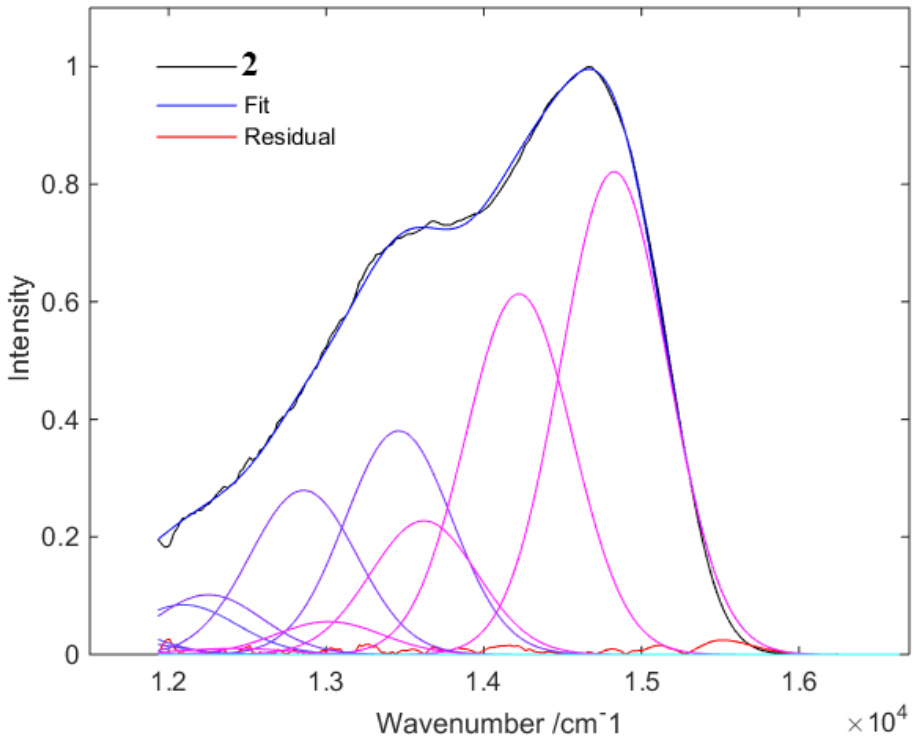


**Figure S11.** Spectral component analysis for **2** in MeOH:EtOH (1:4) glass at 77 K excited at the MLCT maxima with 495 nm light.

## TRANSIENT ABSORPTION SPECTRA

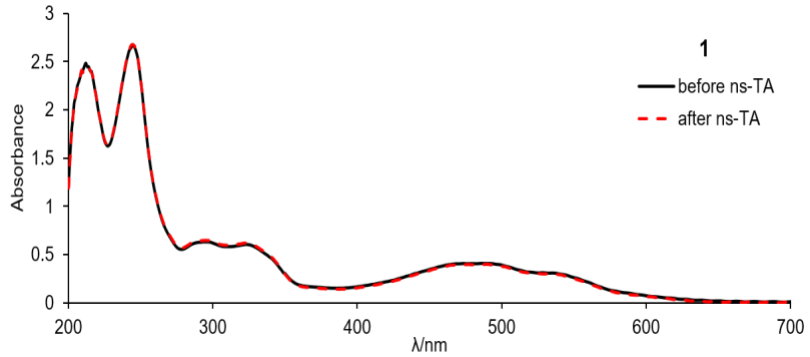


**Figure S12.** Stability of absorbance of **1** under ns-TA conditions.

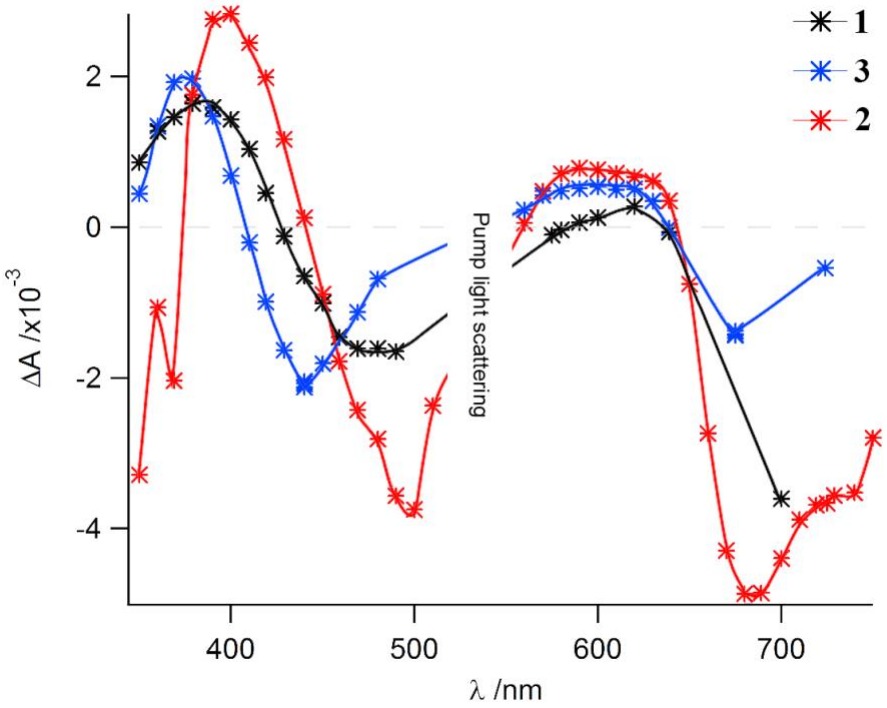


**Figure S13.** Nanosecond transient absorption spectra probed at recorded in MeOH:EtOH (1:4) glass at 77 K and excited with 532 nm light for **1**, **3**, and **2**. The region around 532 nm were not measured due to scattering from the glass. The negative signal above 700 nm is due to spontaneous emission.

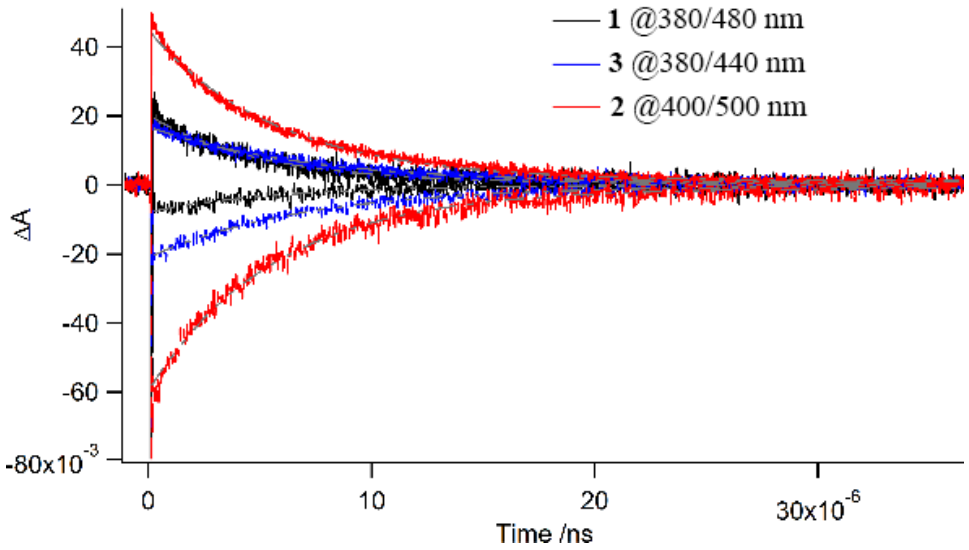


**Figure S14.** ns transient absorption kinetic traces recorded in MeOH:EtOH (1:4) glass at 77 K for **1**, **3**, and **2**, excited at 532 nm and corresponding biexponential fit (grey dashed lines).

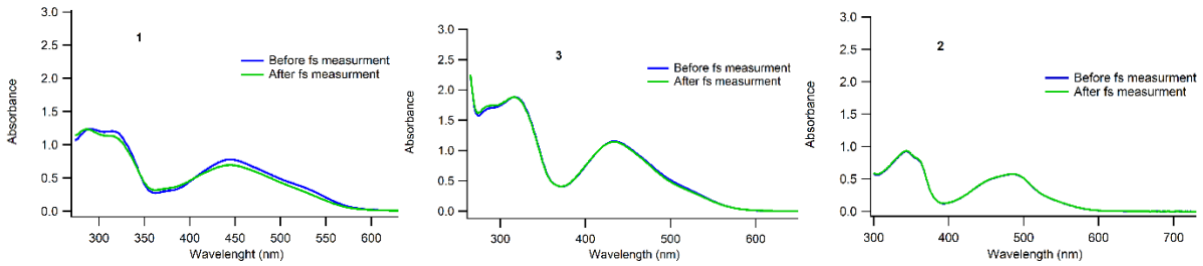


**Figure S15.** Stability of absorbance of each complex under fs-TA conditions.

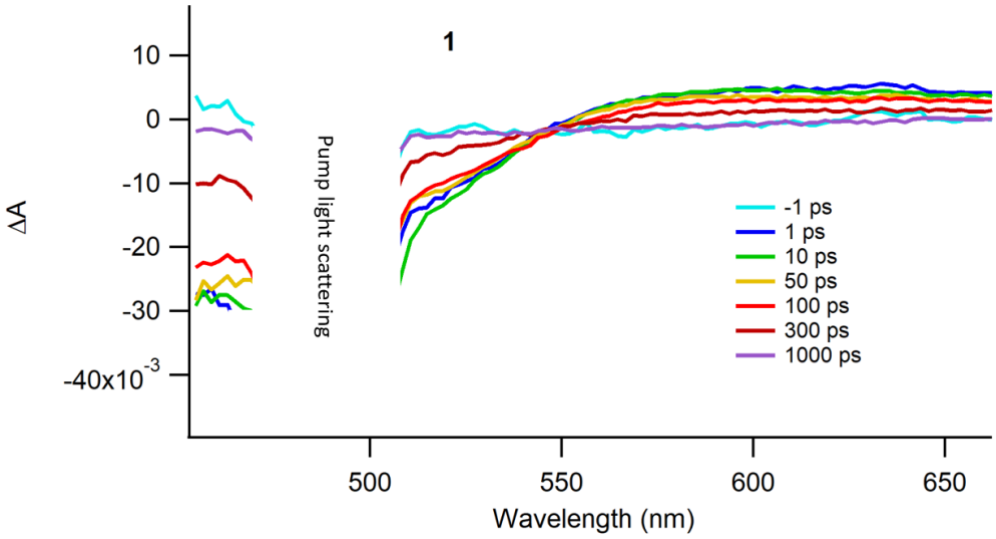


**Figure S16.** fs transient absorption spectra excited at 490 nm for **1** recorded in MeCN. The region around 490 nm is not shown due to scattering from the pump light.

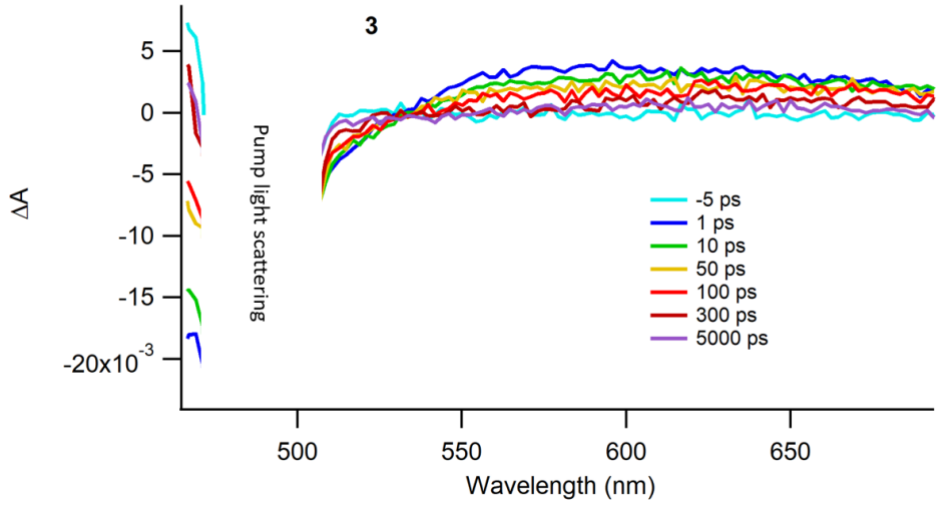


**Figure S17.** fs transient absorption spectra excited at 490 nm for **3** recorded in MeCN. The region around 490 nm is not shown due to scattering from the pump light.

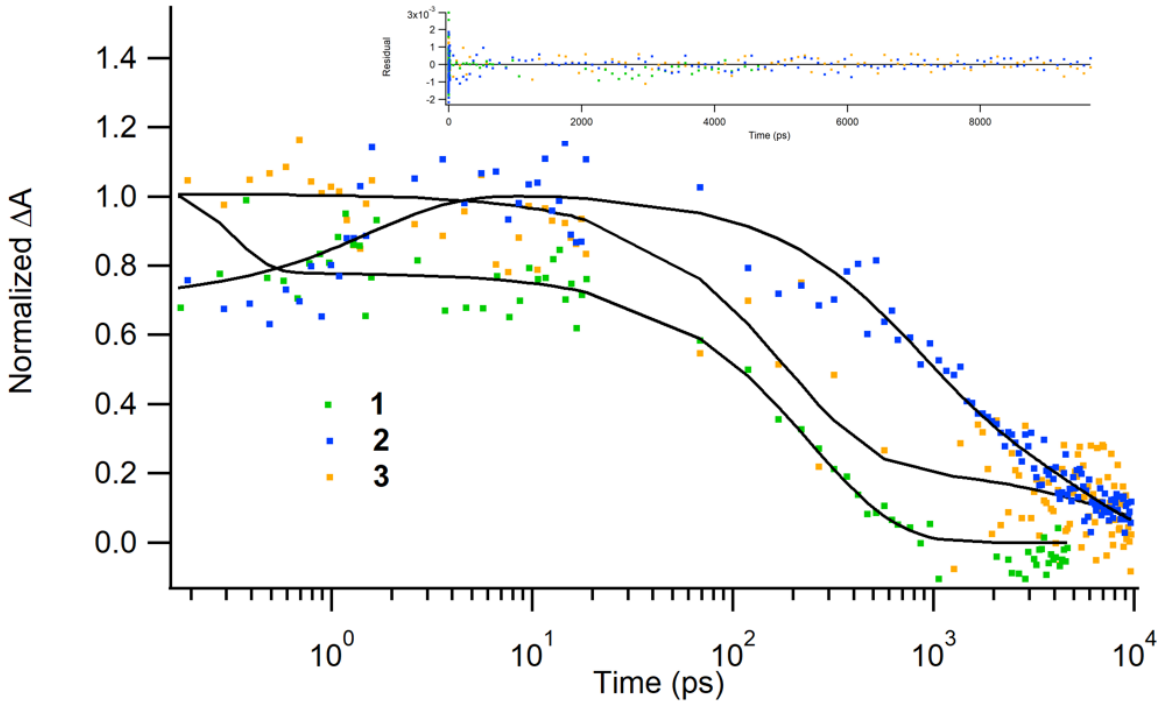


**Figure S18.** Representative single wavelength fs-TA decays from the MLCT excited state absorption band of the complexes and corresponding biexponential fit. Excited at 490 nm. ΔA recorded at 610 nm for **1**, 625 for **2** and **3**. The. The inset shows the residuals.

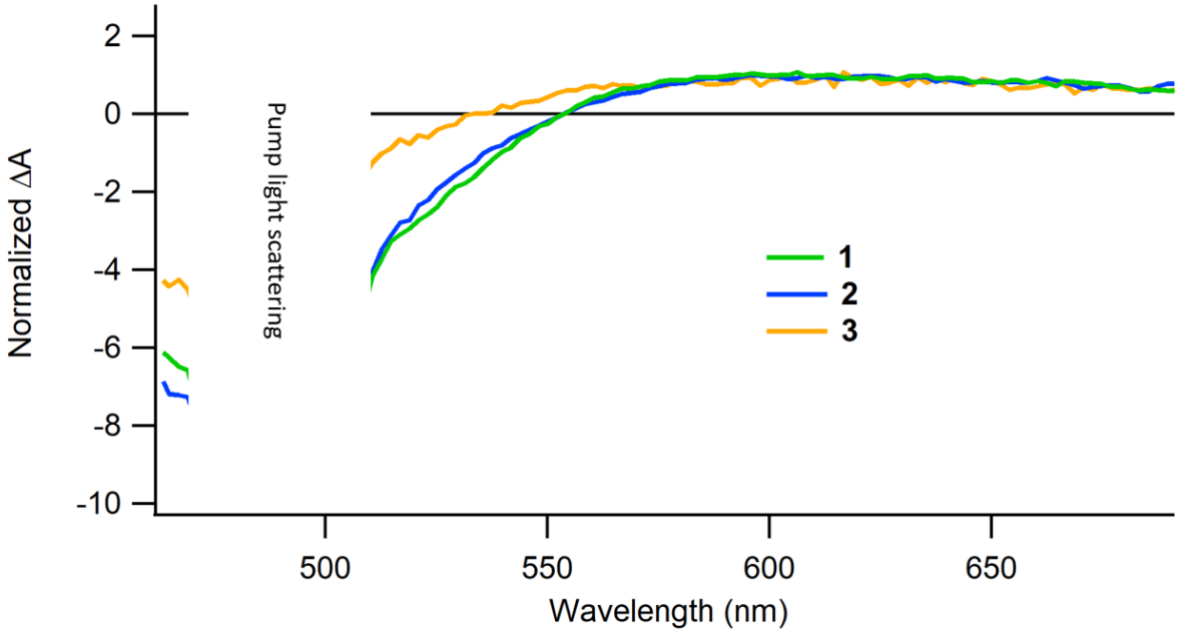


**Figure S19.** Normalized fs TA-spectra for compounds **1-3** at 10 ps after excitation. The spectra display characteristic MLCT features.

## CL– REACTIVITY

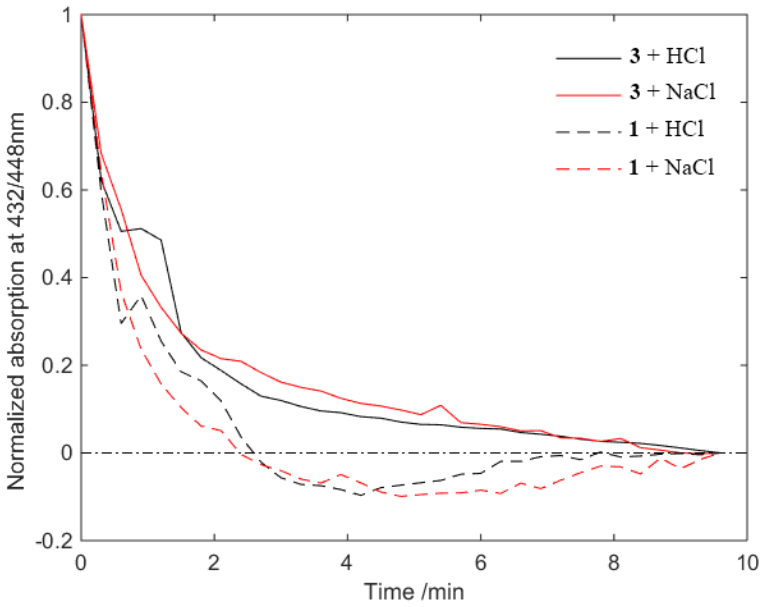


**Figure S20.** Normalized absorption spectra recorded for **3** (at 432 nm) and **1** (at 448 nm) following irradiation with broad band visible light (short-pass filtered at 455 nm) in water with either 0.01M HCl or 0.01M NaCl.

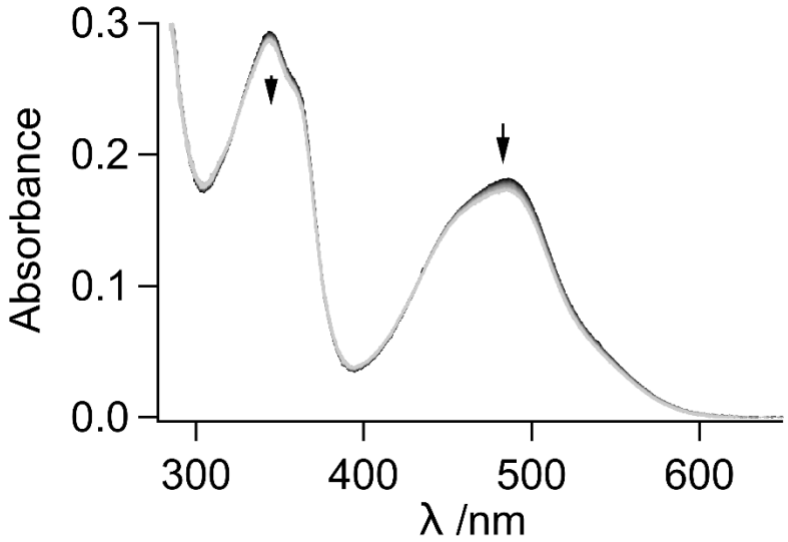


**Figure S21.** Prolonged irradiation of **2** with multiple equivalents of HCl/complex.

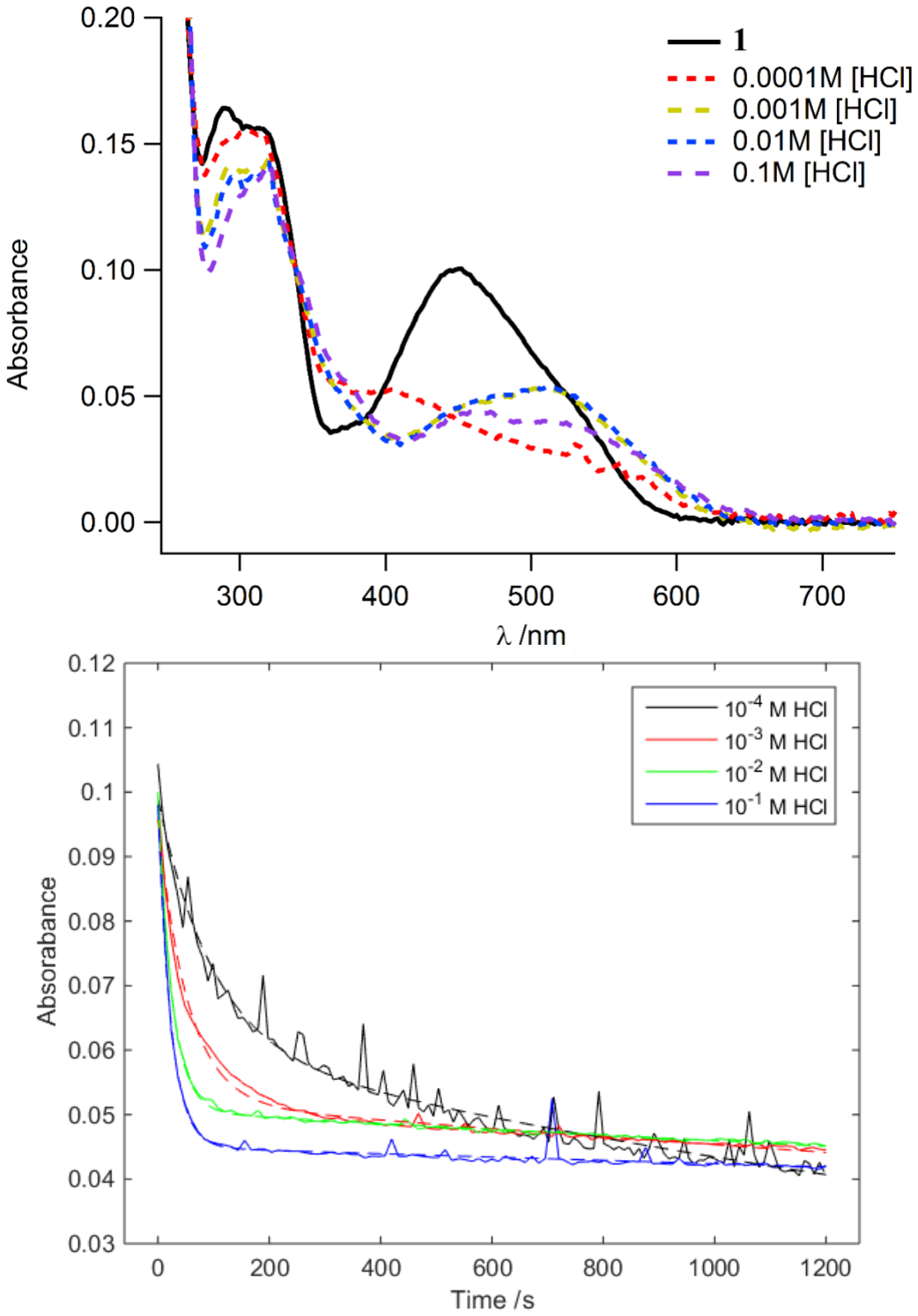


**Figure S22.** Photolysis of **1** in water with varying concentration of HCl. (Top panel) initial and final spectra, and (bottom panel) time trace at $\lambda_{max}$.

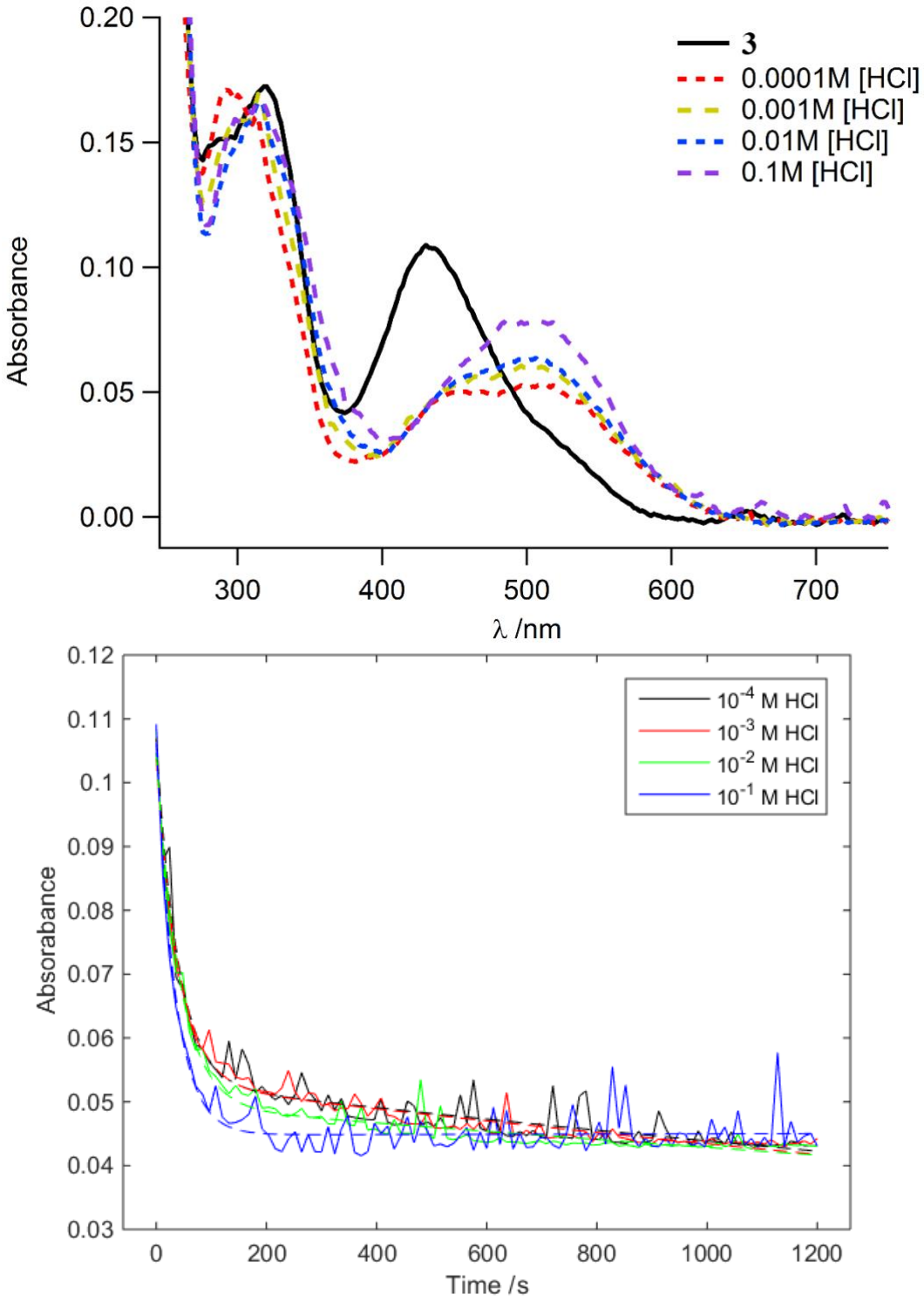


**Figure S23.** Photolysis of **3** in water with varying concentration of HCl. (Top panel) initial and final spectra, and (bottom panel) time trace at $\lambda_{max}$.

**Table S1.** Bi-exponential fitting parameters in photolysis experiment for **1**and **3**. Fitted to $y = a \times e^{-k_1 t} + b \times e^{-k_2 t}$

| **1** | | | | |
|---|---|---|---|---|
| [HCl] /M | a | k1 /×10$_3$ s$^{-1}$ | b | k2 /×10$_3$ s$^{-1}$ |
| 0.0001 | 0.039 | 10.2 | 0.060 | 0.327 |
| 0.001 | 0.044 | 18.7 | 0.052 | 0.134 |
| 0.01 | 0.049 | 39.7 | 0.051 | 0.094 |
| 0.1 | 0.053 | 42.8 | 0.045 | 0.060 |
| **3** | | | | |
| [HCl] /M | a | k1 /s$^{-1}$ | B | k2 /s$^{-1}$ |
| 0.0001 | 0.054 | 25.7 | 0.053 | 0.019 |
| 0.001 | 0.051 | 24.9 | 0.053 | 0.020 |
| 0.01 | 0.055 | 23.8 | 0.049 | 0.014 |
| 0.1 | 0.062 | 29.3 | 0.045 | -0.0005 |

**DFT**

| | $^3$GS | $^3$MLCT | $^3$MC |
|---|---|---|---|
| **1** | 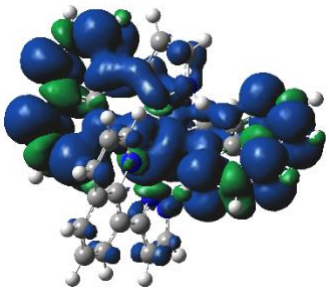 | 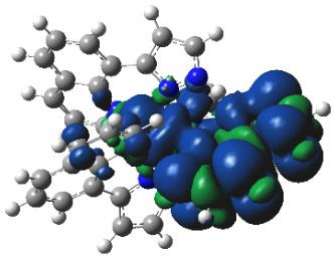 | 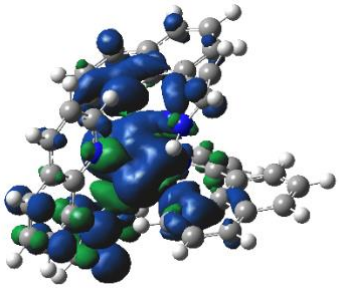 |
| **3** | 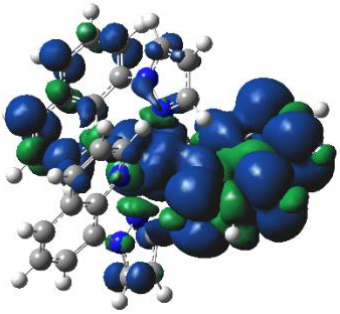 | 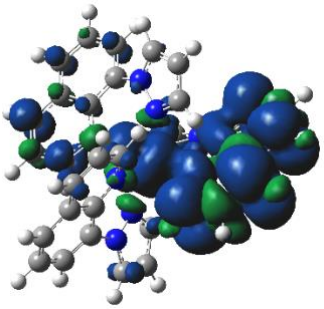 | 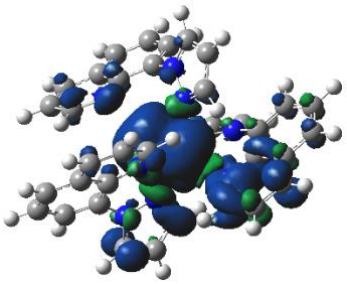 |
| C-Ra **2** | 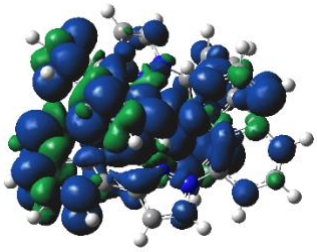 | 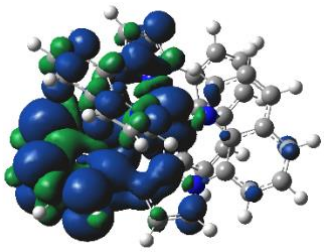 | 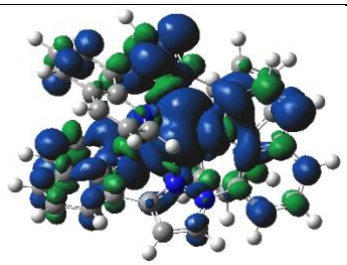 |
| C-Sa **2** | 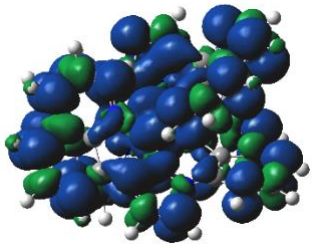 | 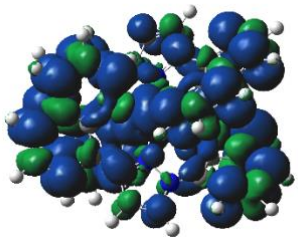 | 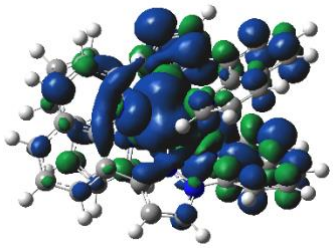 |

**Figure S24.** The triplet spin densities at the GS, MLCT, and MC optimized geometries.

| | | | |
|---|---|---|---|
| **1** | 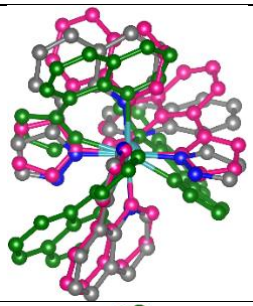 | C-Ra<br>**2** | 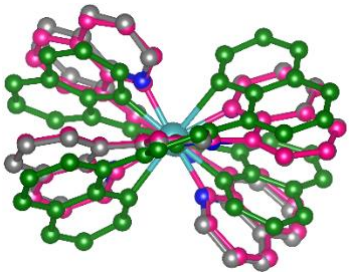 |
| **3** | 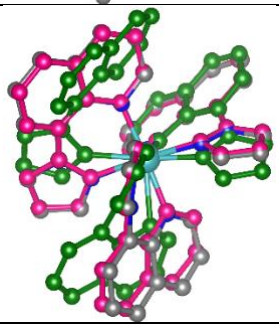 | C-Sa<br>**2** | 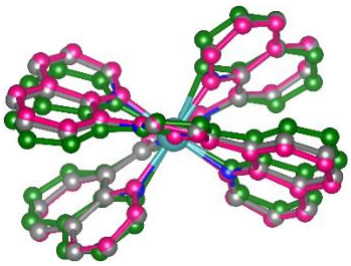 |

**Figure S25.** Overlaid fully optimized geometries GS, MLCT (pink), and MC (green).

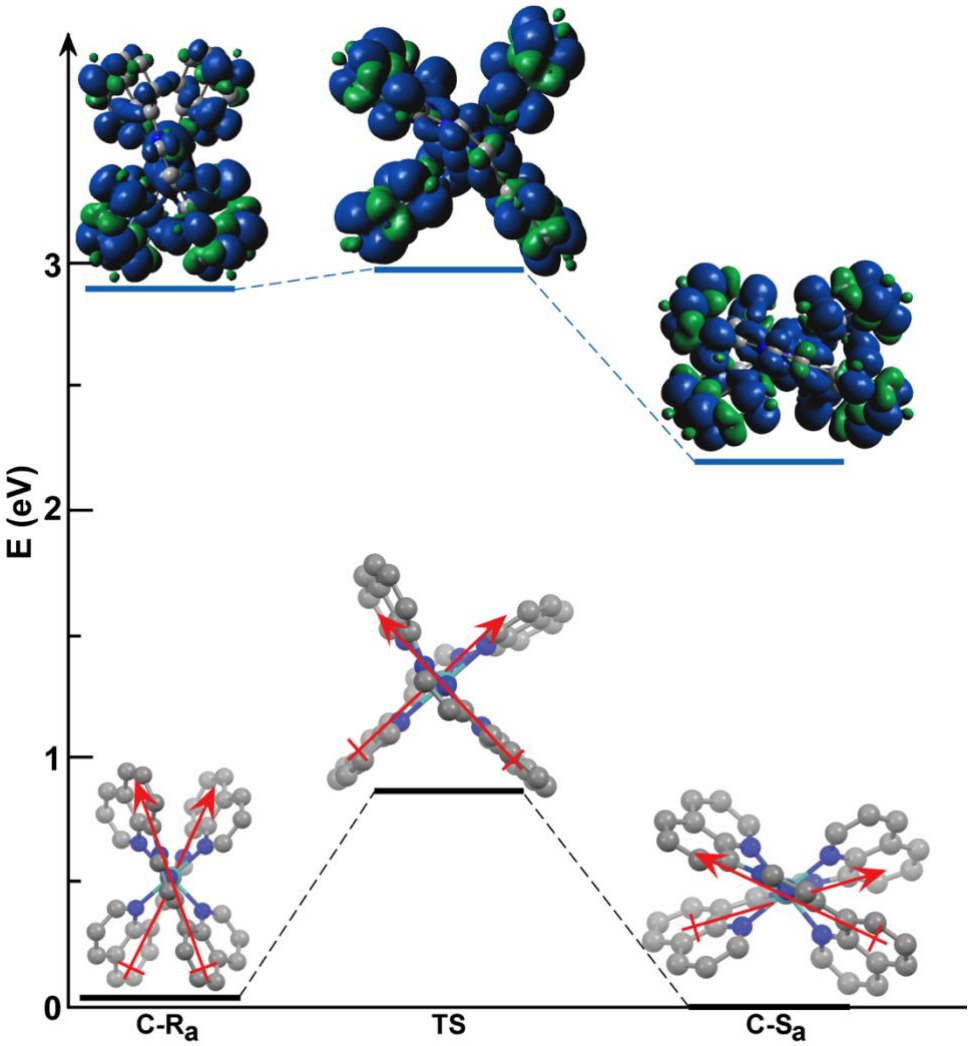


**Figure S26.** Interconversion between the C-Ra and C-Sa isomers of **2** on the ground state surface and vertical triplets above.

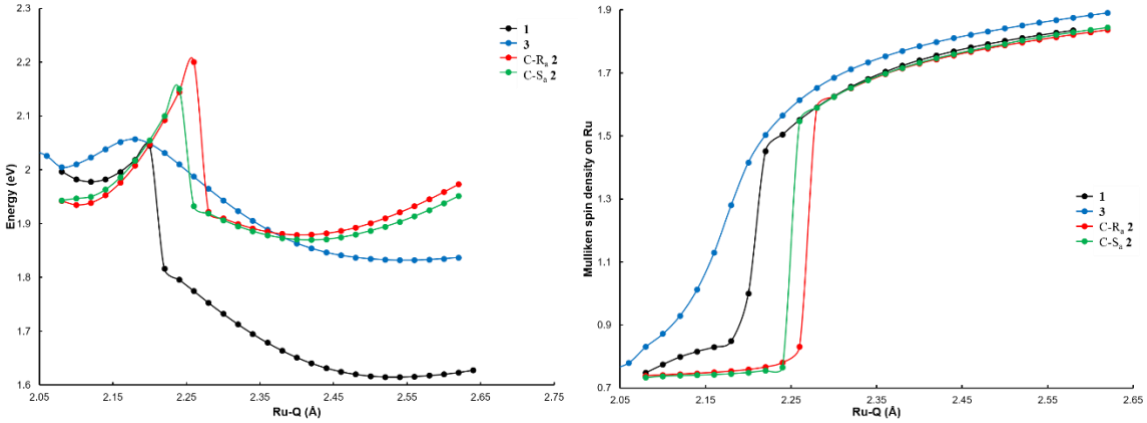


**Figure S27.** Triplet potential energy (left) and spin (right) slices along Ru-(N)Quinoline bond distances for **1**, **3** and the C-Ra and C-Sa isomers of **2** with only the Ru-Q bonds constrained and the rest of the complex optimized for each point.